Heat Mass Transfer (2013) 49:601–616
DOI 10.1007/s00231-012-1106-7

ORIGINAL

A numerical and experimental study of natural convective heat transfer from an inclined isothermal square cylinder with an exposed top surface

Abdulrahim Kalendar · Patrick H. Oosthuizen

Received: 5 April 2012 / Accepted: 11 December 2012 / Published online: 18 January 2013

Abstract Natural convective heat transfer from an isothermal inclined cylinder with a square cross-section which have an exposed top surface and is, in general, inclined at an angle to the vertical has been numerically and experimentally studied. The cylinder is mounted on a flat adiabatic base plate, the cylinder being normal to the base plate. The numerical solution has been obtained by solving the dimensionless governing equations subject to the boundary conditions using the commercial cfd solver, FLUENT. The flow has been assumed to be symmetrical about the vertical center-plane through the cylinder. Results have only been obtained for Prandtl number of 0.7. Values of inclination angle between 0° and 180° and a wide range of Rayleigh number and the dimensionless cylinder width, $W = w/h$, have been considered. The effects of Dimensionless widths, Rayleigh numbers, and inclination angles on the mean Nusselt number for the entire cylinder and for the mean Nusselt numbers for the various surfaces that make up the cylinder have been examined. Empirical equations for the heat transfer rates from the entire cylinder have been derived.

List of symbols

A_{total}	Dimensionless surface area of heated cylinder
A_{side}	Dimensionless surface area of vertical portion of heated cylinder
A_{top}	Dimensionless surface area of horizontal top of heated cylinder
A	Surface area of square cylinder (m^2)
c	Specific heat of material from which model is made (KJ Kg^{-1} K^{-1})
g	Gravitational acceleration (m s^{-2})
h	Height of heated cylinder (m)
h_t	Total heat transfer coefficient (W m^{-2} K^{-1})
h_c	Convective heat transfer coefficient (W m^{-2} K^{-1})
h_{cd}	Conductive heat transfer coefficient (W m^{-2} K^{-1})
h_r	Radiation heat transfer coefficient (W m^{-2} K^{-1})
k	Thermal conductivity of fluid (W m^{-1} K^{-1})
m	Mass of model (Kg)
Nu	Mean Nusselt number based on h and on $(T_w - T_F)$
Nu_{memp}	Mean Nusselt number given by correlation equation
Nu_0	Mean Nusselt number when edge effects are negligible
$Nu_{L(Top)}$	Local Nusselt number based on h and on $(T_w - T_F)$
Nu_{side}	Mean Nusselt number for heated left, right, and front side surfaces of square cylinder
Nu_{left}	Mean Nusselt number for heated vertical left side surface of square cylinder
Nu_{right}	Mean Nusselt number for heated vertical right side surface of square cylinder
Nu_{front}	Mean Nusselt number for heated front vertical side surface of square cylinder
Nu_{Top}	Mean Nusselt number for heated top surface of cylinder
Pr	Prandtl number
P	Dimensionless pressure

A. Kalendar (✉)
Department of Mechanical Power and Refrigeration,
College of Technological Studies-PAAET,
Shuwaikh, Kuwait
e-mail: kalendar@hotmail.com

P. H. Oosthuizen
Department of Mechanical and Materials Engineering,
Queen's University, Kingston, ON K7L 3N6, Canada

p	Pressure (Pa)
p_F	Pressure in undisturbed fluid (Pa)
Q_{total}	Mean heat transfer rate over heated surface of cylinder (W)
Q_{Top}	Mean heat transfer rate over top side of heated cylinder (W)
q'	Mean heat transfer rate per unit area over heated surfaces of cylinder (W m^{-2})
q'_{left}	Mean heat transfer rate per unit area over left portion of heated square cylinder (W m^{-2})
q'_{right}	Mean heat transfer rate per unit area over right portion of heated square cylinder (W m^{-2})
q'_{front}	Mean heat transfer rate per unit area over front portion of heated square cylinder (W m^{-2})
q'_{top}	Mean heat transfer rate per unit area over top side of heated square cylinder (W m^{-2})
Ra	Rayleigh number based on h and temperature differences
T	Temperature (K)
T_F	Fluid temperature (K)
T_w	Temperature of surface of square cylinder (K)
T_{wavg}	Average wall temperature of surface of cylinder (K)
T_e	Model final temperature (K)
T_i	Model initial temperature (K)
t	Time to go from T_i to T_e (s)
u_r	Reference velocity (m s^{-1})
U_X	Dimensionless velocity component in X direction
u_x	Velocity component in x direction (m s^{-1})
U_Y	Dimensionless velocity component in Y direction
u_y	Velocity component in y direction (m s^{-1})
U_Z	Dimensionless velocity component in Z direction
u_z	Velocity component in z direction (m s^{-1})
W	Dimensionless width of cylinder (=w/h)
w	Width of cylinder (m)
X	Dimensionless horizontal coordinate
x	Horizontal coordinate (m)
Y	Dimensionless horizontal coordinate
y	Horizontal coordinate (m)
z	Vertical coordinate (m)
Z	Dimensionless vertical coordinate
α	Thermal diffusivity (m^2 s^{-1})
β	Bulk coefficient (K^{-1})
σ	Stefan–Boltzman constant
ε	Emissivity of the model
v	Kinematic viscosity (m^2 s^{-1})
θ	Dimensionless temperature
φ	The angle of inclination of the cylinder relative to the vertical (°)

1 Introduction

Natural convective heat transfer from an isothermal inclined cylinder with a square cross-section which have an exposed top surface and is, in general, inclined at an angle to the vertical has been numerically and experimentally studied. Some electrical and electronic component cooling problems can be approximately modeled as involving natural convective heat transfer from an isothermal inclined cylinder with a square cross-section mounted on a flat adiabatic base plate. The cylinder has an exposed top surface which is also isothermal and has the same temperature as that of the vertical heated side surfaces. This flow situation, which is considered here, is shown in Fig. 1. The heat transfer from the surface of the cylinder at various angles of inclination between vertically upwards and vertically downwards, as in Fig. 2, has been numerically and experimentally investigated. One of the main aims of the present work was to determine how the cross-sectional size-to-height ratio of the square cylinder, i.e., w/h, influences the mean heat transfer rate from the cylinder at various angles of inclination.

Natural convection from vertical slender circular cylinders has been studied for many years. Reviews of early work were provided by Ede [1], Burmeister [2], and Jaluria [3]. Cebeci [4] gives numerical results for Prandtl numbers from 0.01 to 100, extending earlier work that had been for $Pr = 1$ and 0.72. This work was further extended by Lee et al. [5]. Integral method results were obtained by LeFevre and Ede [6]. The effect of Prandtl number was further studied by Crane [7]. There have been several more recent

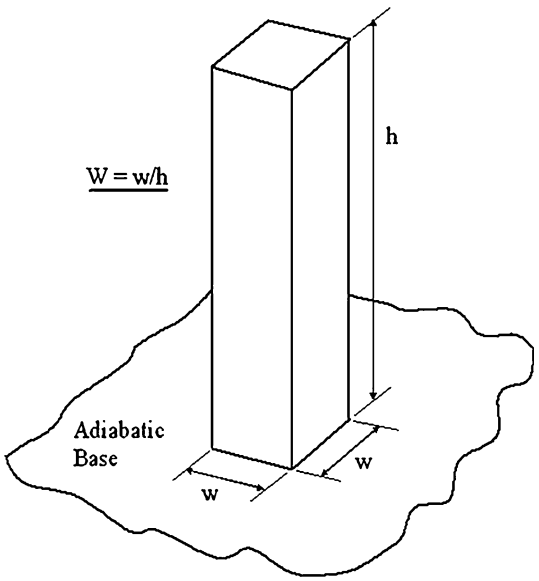

Fig. 1 Flow situation considered

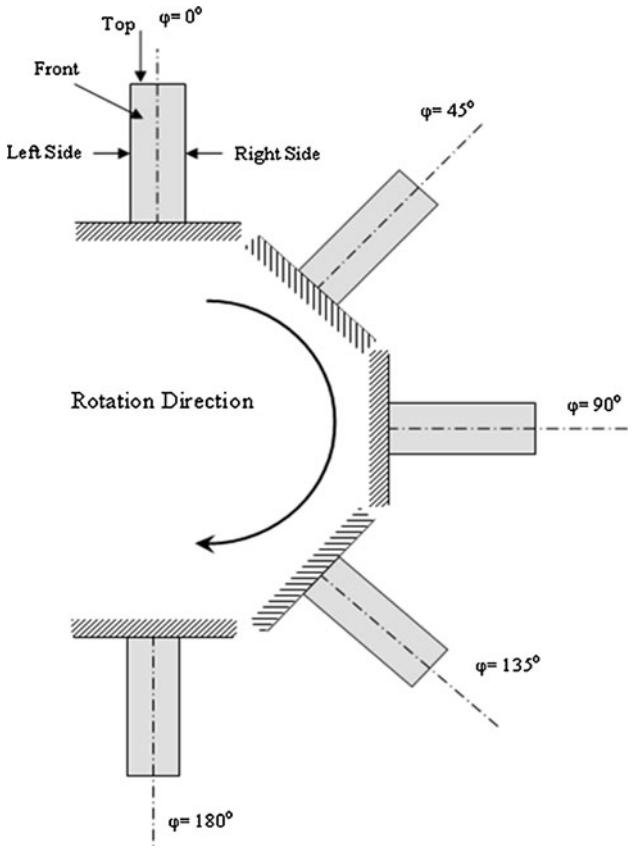

Fig. 2 Definition of inclination angle and faces

studies that have further extended this earlier work typical of these being that of Kimura et al. [8] and Oosthuizen [9, 10]. Typical of the experimental studies of natural convective heat transfer from vertical circular cylinders are those of Jarall and Campo [11], Welling et al. [12] and Fukusawa and Iguchi [13]. Cylinders with exposed top inclined at an angle to the vertical have received attention by Oosthuizen [14, 15].

Some studies of natural convective heat transfer from inclined cylinders have been undertaken. In very early study such as Koch [16] and Farber and Rennat [17]. Few studies however have been concerned with short inclined cylinders such as Oosthuizen [18], Eckert and Jackson [19], Al-Arabi and Salman [20], Al-Arabi and Khamis [21], Chand and Vir [22], Oosthuizen and Mansingh [23] and Oosthuizen and Paul [24].

Some studies of natural convective heat transfer from inclined square cylinders have been undertaken. An experimental study of natural convective heat transfer from an isothermal vertical short and slender square cylinder to air, where the top and bottom surfaces were insulated, were obtained using a lumped capacitance method by Popiel and Wojtkowiak [25]. Even with their widest square cylinder, the mean Nusselt numbers were higher than given by the correlation equation for the wide flat plate, this being especially true at low Rayleigh numbers. Experiments were carried out by Al-Arabi and Sarhan [26] to measure the average natural convection heat transfer rate from the outside surface of isothermal square cylinders of different length and side-lengths at different angle of inclination between 0° and 90° to the vertical in both laminar and turbulent regions. The heat transfer rates from the side surfaces of the square cylinder where the top and bottom ends are insulated were measured. The heat transfer rate was found to depend on side-length and the inclination angle. They found that due to the presence of edge effects, the heat transfer coefficient always exceeded that which would occur under the same conditions with a vertical plate. They also suggested general correlation equations. Natural convective heat transfer from an isothermal vertical square cylinder with exposed upper surface in air mounted on a flat adiabatic base was studied by Oosthuizen [27]. His solution has values of the parameters *w/h* between 0.1 and 1, Rayleigh number between 1×10^4 and 1×10^7, and Prandtl number of 0.7. His results showed that at the lower values of Rayleigh number and *w/h* considered the mean Nusselt number increases with decreasing *w/h*, while at larger values of Rayleigh number and *w/h* the Nusselt number is essentially independent of *w/h*. Also the mean Nusselt number for the heated top surface was shown to be much lower than that for the vertical side surfaces. He provide a correlation equations for the top and the side surfaces.

Heat transfer from cylinders with a square or rectangular cross-section has mainly been studied from the point of view of their use in pin–fin heat sinks. Typical of these studies are those of Starner and McManus [28], Welling, and Wooldridge [29], Harahap, and McManus [30], Leung, et al. [31], Leung and Probert [32], Yuncu and Anbar [33], Mobedi and Yuncu [34], Harahap, and Rudianto [35], Sahray, et al. [36], Harahap, et al. [37], Yazicioglu, and Yancu [38], and Sahray, et al. [39]. The present study is an extension of that described in Refs. [40–42].

2 Experimental apparatus and procedures

To study the natural convective heat transfer from a square cylinder which is inclined at an angle to the vertical, a free convection test chamber in which the model could be mounted was designed and constructed. Figure 3 shows a schematic front view of the experimental apparatus. The experimental test chamber had a size of 120 cm height × 25 cm width × 30 cm depth of Plexiglass. It was opened from the top and bottom mounted on a horizontal floor so it surrounds the test section. The volume of the test chamber was large enough to ensure that it did not interfere

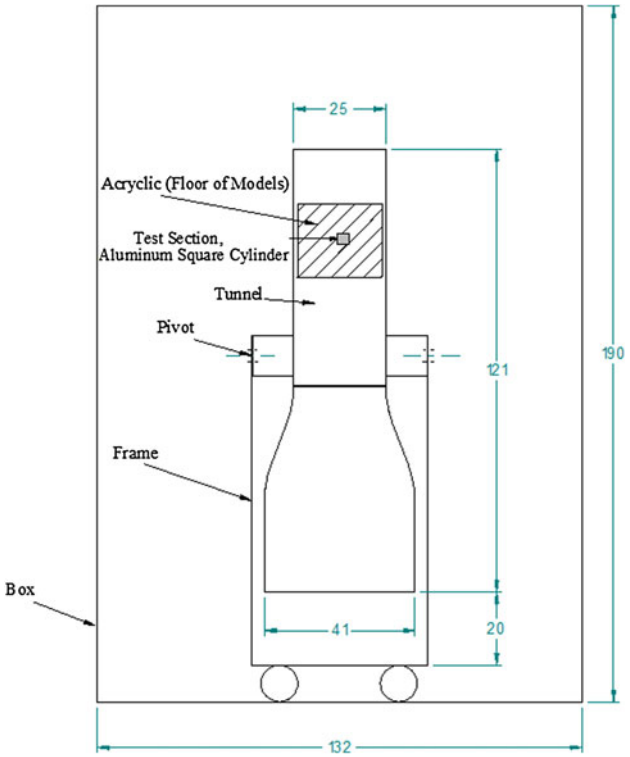

Fig. 3 Experimental apparatus, dimensions are in cm

with the flow over and heat transfer rates from the model. The test chamber was constructed using transparent acrylic plates and constructed in such a way that it can be rotated around a fixed horizontal axis, in this way allowing the inclination angle of the test section to be changed. Furthermore the test chamber is placed in a bigger box 190 cm height × 135 cm width × 125 cm depth which was vented to the room. This arrangement ensures that no external disturbances in the room air or short term temperature changes in the room interfere with the experiments.

The active component of the test apparatus was the solid aluminum square cylinder models used in the experiments, the model sizes are given in Table 1. The square cylinder model has a height of h and cross-sectional width w. The aspect ratio of the models used w/h range from 0.25 to 1. The bottom surface of the model is attached to a large base made of plexiglass 29 cm in length, 23.5 cm in width, and 1.2 cm thick. The end of the model in contact with this base being internally chamfered in order to reduce the contact area between the model and the sheet in order to reduce the conduction heat transfer from the model to the base. A series of small diameter holes were drilled longitudinally to various depths into the models. Seven thermocouples type-T 0.25 mm in diameter were inserted into these holes in various locations were used to measure temperatures. The thermocouples were monitored using a data acquisition system manufactured by TechmaTron

Table 1 Model dimensions

Model no.	Width (w) mm	Height (h) mm	$W = w/h$
1	25.4	25.4	1.0
2	25.4	33.3	0.75
3	25.4	50.2	0.50
4	25.4	100.1	0.25

Instrument (model USB-TC) which was self calibrating and that in turn was connected to a personal computer. The thermocouples with the data acquisition system were calibrated in a digital temperature controller water bath manufactured by VWR model 1166D, with the calibrated reference thermometer manufactured by Guildline Instruments Company model 9535/01,02,03 between 20 and 100 °C and their output are less than ±0.5 °C of the actual temperature. As noted before the model assemblies could be mounted inside the test chamber as shown in Fig. 3. This allowed the models to be set at any angle to the vertical.

2.1 Derivation of the experimental results

The heat transfer rates were determined using the transient method, i.e., by heating a model being tested and then measuring its temperature–time variation while it cooled. In an actual test, the model being tested was set at a required angle and then heated in an oven to a temperature of about 140 °C. The model temperature variation with time was then measured while it cooled from 95–40 °C. Tests and approximate calculations indicated that, because the Biot numbers existing during the tests were very small less than 1×10^{-4} which meets the general requirement for applicability of the lumped system method of $\mathrm{Bi} < 10^{-1}$. As a result of low Biot number, the temperature of the aluminum models remained effectively uniform at any given instant of time during the cooling process. The overall heat transfer coefficient could then be determined from the measured temperature–time variation using the usual procedure, i.e., the temperature variation of the model was therefore related to the time by:

$$\left(\frac{h_t A}{mC}\right) t = \ln\left(\frac{T_i - T_\infty}{T_e - T_\infty}\right) \tag{1}$$

Hence, h_t could be determined from the measured variation of $ln(T_i - T_\infty)/(T_e - T_\infty)$ with t, and known value of (A/mc).

The value of h_t so determined is, of course, made up of the convective heat transfer to the surrounding air, the radiant heat transfer to the surroundings and the conduction from the model to the base. The radiant heat transfer could be allowed for by calculation using the known emissivity

0.1 of the polished surface of the aluminum models. So the radiant heat transfer coefficient could be calculated as,

$$h_r = \varepsilon\,\sigma\left(T_{w_{avg}} + T_\infty\right)\left(T_{w_{avg}}^2 + T_\infty^2\right) \quad (2)$$

The conduction heat transfer to the base was calculated by fully covering the models with Styrofoam insulation and using the transient method as described before. The convective rate of the heat coefficient by convection is calculated as:

$$h_c = h_t - h_r - h_{cd} \quad (3)$$

The estimated values of convection, conduction and radiation heat transfer coefficients depend on the size of the experimental model, orientation and Rayleigh number, e.g. when the Rayleigh number is equal to 5.89×10^4 and $W = 1$, then $h_c \approx 66.8$ %, $h_{cd} \approx 29.9$ % and $h_r < 3.3$ % while when the Rayleigh number is equal to 3.62×10^6 and $W = 0.25$, then $h_c \approx 78$ %, $h_{cd} \approx 17.4$ % and $h_r < 4.6$ % of the total heat transfer.

The dimensional analysis indicates that natural convection heat transfer from short square cylinders inclined at an angle to the vertical depends on Nusselt number, *Nu*, Rayleigh number, *Ra*, the ratio of the width to the height of the square cylinder, *W,* and the inclination angle to the vertical, φ, i.e.;

$$Nu = f(Ra, W, \varphi) \quad (4)$$

where *Ra* is defined as,

$$Ra = \frac{\beta g(T_{w_{avg}} - T_F)h^3}{\nu\alpha} \quad (5)$$

and the average Nusselt number is defined as usual as:

$$Nu = \frac{h_c h}{k} \quad (6)$$

In expressing the experimental results in dimensionless form, all air properties in the Nusselt and Rayleigh numbers have been evaluated at the mean film temperature $(T_{w_{avg}} + T_F)/2$ existing during the test.

The uncertainty in the present experimental values of Nusselt number arises due to uncertainties in the temperature measurements, non-uniform heating, temperature differences in the model during cooling, and uncertainties in the corrections applied for conduction heat transfer through the base. Therefore, an uncertainty analysis was performed by applying the estimation method proposed by Moffat [43, 44]. The uncertainty in the average Nusselt number was found to be a function of temperature, the angle of inclination and the size of the experimental model used. Overall, the uncertainty in the average Nusselt number was estimated to be less than ±12 % for selected time interval, and the scatter in the experimental data is between ±3 % of the mean values.

Tests were performed with models mounted at various angles of inclination between vertically upwards and vertically downwards as shown Fig. 2. This work will focus on the effect of inclination angle and the aspect ratio of the square cylinder with exposed top surface on the mean heat transfer rate.

3 Numerical solution procedure

The solution domain used in obtaining the numerical solution is shown in Fig. 4. The flow has been assumed to be symmetric about the vertical center plane DEFOTS-IND shown in Fig. 4 and to be steady and laminar. It has also been assumed that the fluid properties are constant except for the density change with temperature which gives rise to the buoyancy forces, this being treated here by using the Boussinesq approach. The governing equations have been written in dimensionless form using the height, *h*, of the cylinder as the length scale and $T_w - T_F$ as the temperature scale, T_w being the temperature of surface of cylinder and T_F being the fluid temperature far from the cylinder. The following reference velocity has been introduced:

$$u_r = \frac{\alpha}{h}\sqrt{Ra\,Pr} \quad (7)$$

where *Pr* is the Prandtl number and *Ra* is the Rayleigh number based on *h*, i.e.:

$$Ra = \frac{\beta g(T_w - T_F)h^3}{\nu\alpha} \quad (8)$$

The following dimensionless variables have then been defined:

$$X = \frac{x}{h}, Y = \frac{y}{h}, Z = \frac{z}{h}, U_X = \frac{u_x}{u_r},$$
$$U_Y = \frac{u_y}{u_r}, U_Z = \frac{u_z}{u_r}, P = \frac{(p - p_F)h}{\mu u_r},$$
$$\theta = \frac{T - T_F}{T_w - T_F} \quad (9)$$

where *T* is the temperature, T_w is the temperature of the hot cylinder walls and T_F is the fluid temperature far from the cylinder. As shown in Fig. 4, the *z*-coordinate is measured along the axis of the cylinder and the *x*- and *y*-coordinate are measured in the plane of the flat adiabatic base plate. In terms of these dimensionless variables and if φ is the angle from the vertical at which the plate is inclined the governing equations are the following:

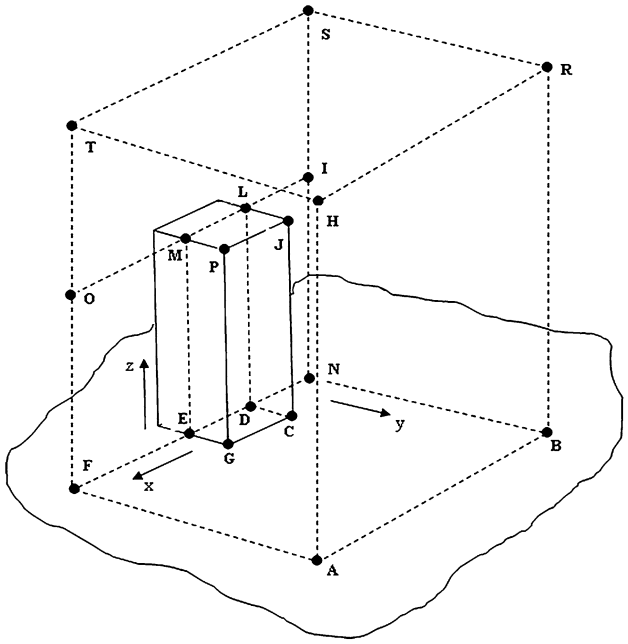

Fig. 4 Solution domain

$$\frac{\partial U_X}{\partial X} + \frac{\partial U_Y}{\partial Y} + \frac{\partial U_Z}{\partial Z} = 0 \tag{10}$$

$$U_X\frac{\partial U_X}{\partial X} + U_Y\frac{\partial U_X}{\partial Y} + U_Z\frac{\partial U_X}{\partial Z} = \sqrt{\frac{Pr}{Ra}}\left(-\frac{\partial P}{\partial X} + \frac{\partial^2 U_X}{\partial X^2} + \frac{\partial^2 U_X}{\partial Y^2} + \frac{\partial^2 U_X}{\partial Z^2}\right) + \theta\sin\varphi \tag{11}$$

$$U_X\frac{\partial U_Y}{\partial X} + U_Y\frac{\partial U_Y}{\partial X} + U_Z\frac{\partial U_Y}{\partial X} = \sqrt{\frac{Pr}{Ra}}\left(-\frac{\partial P}{\partial Y} + \frac{\partial^2 U_Y}{\partial X^2} + \frac{\partial^2 U_Y}{\partial Y^2} + \frac{\partial^2 U_Y}{\partial Z^2}\right) \tag{12}$$

$$U_X\frac{\partial U_Z}{\partial X} + U_Y\frac{\partial U_Z}{\partial Y} + U_Z\frac{\partial U_Z}{\partial Z} = \sqrt{\frac{Pr}{Ra}}\left(-\frac{\partial P}{\partial Z} + \frac{\partial^2 U_Z}{\partial X^2} + \frac{\partial^2 U_Z}{\partial Y^2} + \frac{\partial^2 U_Z}{\partial Z^2}\right) + \theta\cos\varphi \tag{13}$$

$$U_X\frac{\partial \theta}{\partial X} + U_Y\frac{\partial \theta}{\partial Y} + U_Z\frac{\partial \theta}{\partial Z} = \frac{1}{\sqrt{RaPr}}\left(\frac{\partial^2 \theta}{\partial X^2} + \frac{\partial^2 \theta}{\partial Y^2} + \frac{\partial^2 \theta}{\partial Z^2}\right) \tag{14}$$

Because the flow has been assumed to be symmetric about the vertical center-plane of the cylinder, the domain used in obtaining the solution is as shown in Fig. 4. The assumed boundary conditions on the solution in terms of the dimensionless variables are that for all the cylinder surfaces the dimensionless velocity components are all equal to zero and the dimensionless temperature is equal 1. On the adiabatic base the assumed boundary conditions are that all dimensionless velocities are equal to zero and that the dimensionless temperature gradient normal to all surfaces is equal to 0. On the plane of symmetry the dimensionless velocity component normal to the plane is zero and the gradients normal to this plane of the remaining velocity components and temperature are zero. On the outer planes of the solution domain the dimensionless temperature is equal to zero and the velocity components in the plane parallel to the surface are zero. On the upper surface HTSR the boundary conditions are the dimensionless temperature is equal to zero and the pressure is equal to zero. The outer boundary conditions of the solution domain were changed as the domain rotated from 0° to 180°.

The above dimensionless governing equations subject to the boundary conditions discussed above have been numerically solved using the commercial finite-volume solver, FLUENT. In obtaining the numerical results the pressure-based solver was used with the second-order upwind scheme for convective terms in the mass, momentum and energy equations. For pressure discretization, the Presto scheme has been employed while the SIMPLE-algorithm has been used for pressure–velocity coupling discretization. Extensive grid and convergence criterion independence testing was undertaken for all cases studied in the present work. A non-uniform grid distribution is used in the plane perpendicular and parallel to the main flow direction. This indicated that the heat transfer results presented here are to less than 1 % independent of the number of grid points and of the convergence-criterion used. Some typical results obtained here in the grid-independence testing are shown in Tables 2 and 3. These results are for the case of natural convective heat transfer from vertical and inclined square cylinders when dimensionless width, W, is equal to 1. In obtaining the results the number of nodes used was 1,191,641. Close to the square cylinder, the number of grid points or control volumes is increased to enhance the resolution and accuracy. The results in Tables 2 and 3 show that the mean Nusselt number for the surfaces that make up the cylinder for the selected number of nodes are to less than 1 % independent of the number of grid points. The effect of the distances of the outer surfaces of the solution domain (i.e., surfaces BRSN, AHTOF, ABRH, and HRST in Fig. 4) from the heated surfaces was also examined and the positions used in obtaining the results discussed here were chosen to ensure that the heat transfer results were independent of this positioning to within 1 %.

The mean Nusselt number for the heated cylinder is defined by:

$$Nu = \frac{\bar{q}'h}{k(T_w - T_F)} \tag{15}$$

where $\bar{q}'$ is the mean heat transfer rate per unit area from the entire surface of the cylinder. Similarly the mean

Table 2 Results for the mesh independence study for $W = 1$, $Ra = 1E6$ and $\varphi = 0°$, 90° and 180°

Rayleigh no.	Tilt angle	No. of nodes	Nu_{left}	Nu_{right}	Nu_{Front}	Nu_{Top}	Nu_{Total}
1×10^6	0°	532,408	17.485	17.57	17.633	6.11	15.298
		628,730	17.284	17.344	17.536	6.036	15.147
		764,791	17.117	17.159	17.575	6	15.085
		837,385	17.026	17.072	17.223	5.932	14.895
		930,109	16.933	16.99	17.116	5.955	14.822
		1,040,126	16.648	16.648	16.578	5.85	14.46
		1,191,641	16.607	16.607	16.545	5.871	14.435
		1,223,280	16.595	16.595	16.54	5.88	14.43
1×10^6	90°	930,109	6.288	12.446	15.327	15.955	13.068
		1,040,126	6.826	12.231	14.913	16.389	13.054
		1,191,641	6.877	12.184	14.891	16.397	13.048
		1,223,280	6.895	12.178	14.892	16.398	13.051
1×10^6	180°	930,109	14.195	14.254	14.246	14.102	14.21
		1,040,126	14.076	14.076	14.033	14.228	14.09
		1,191,641	14.054	14.054	14.004	14.127	14.05
		1,223,280	14.063	14.063	14.028	14.183	14.07

Table 3 Results for the mesh independence study for $W = 1$, $Ra = 1E4$ and $\varphi = 0°$, 90°, 180°

Rayleigh no.	Tilt angle	No. of nodes	Nu_{left}	Nu_{right}	Nu_{Front}	Nu_{Top}	Nu_{Total}
1×10^4	0°	930,109	5.365	5.363	5.296	2.513	4.766
		1,040,126	5.339	5.339	5.353	2.486	4.774
		1,191,641	5.342	5.342	5.355	2.485	4.776
		1,223,280	5.346	5.346	5.352	2.485	4.777
1×10^4	90°	930,109	2.01	5.122	5.036	5.567	4.554
		1,040,126	2.027	5.101	5.023	5.5106	4.537
		1,191,641	2.036	5.1103	5.046	5.484	4.544
		1,223,280	2.032	5.102	5.023	5.5105	4.538
1×10^4	180°	930,109	4.362	4.357	4.326	5.934	4.661
		1,040,126	4.382	4.382	4.382	5.871	4.68
		1,191,641	4.376	4.376	4.375	5.825	4.666
		1,223,280	4.389	4.389	4.383	5.863	4.682

Nusselt numbers for the left, right, front and top side surfaces of the cylinder are defined as follows:

$$Nu_{left} = \frac{q'_{left}\, h}{k(T_w - T_F)} \tag{16}$$

$$Nu_{right} = \frac{q'_{right}\, h}{k(T_w - T_F)} \tag{17}$$

$$Nu_{front} = \frac{q'_{front}\, h}{k(T_w - T_F)} \tag{18}$$

$$Nu_{Top} = \frac{q'_{top} h}{k(T_w - T_F)} \tag{19}$$

where q'_{left}, q'_{right}, q'_{front} and q'_{top} are the mean heat transfer rates per unit area from the left, right, front and top side surfaces of the cylinder respectively.

4 Results

The solution has the following parameters:

1. The Rayleigh number, Ra, based on the 'height' of the heated cylinder, h, and the overall temperature difference $T_w - T_F$
2. The dimensionless width of the cylinder, $W = w/h$
3. The Prandtl number, Pr
4. The inclination angle φ of the cylinder

Because of the applications that motivated this study, results have only been obtained for $Pr = 0.7$. A wide range of the other governing parameters have been considered.

In order to validate the results a comparison between the present experimental results and the correlation equations by Churchill and Chu [45] and Oosthuizen [27] are shown

in Fig. 5. Oosthuizen [27] correlation equation is valid for a vertical isothermal square cylinder with an exposed top surface where the dimensionless width of the cylinder is less than 0.6. Churchill and Chu [45] correlation equation are valid for a wide plate. Good agreement between the correlation equations and the experimental results for isothermal vertical square cylinder for $W = 0.5$ where the heat transfer from the top surface is small compared to the heat transfer from the side surfaces.

Typical variations of numerical and experimental values results of the mean Nusselt number for the entire cylinder, *Nu*, with Rayleigh number, *Ra*, for various values of the dimensionless cylinder width, *W*, at different angles of inclination, φ, between vertically upward and vertically downward are shown in Figs. 6, 7, 8, 9 and 10. These figures show that the mean Nusselt number increases as the Rayleigh number increases and the dimensionless cylinder width decreases for all values of inclination angles considered in this study. The increase in the Nusselt number with decreasing dimensionless cylinder width, *W*, arises from the fact that there is an induced inflow from the edges towards the center of the faces of the square cylinder and this causes the heat transfer rate to be higher near the vertical edges of the square cylinder than it is in the center region of the cylinder. The experimental results given in these Figures seen to be in good agreement with the numerical results and shows the same trends as the numerical results. However it will be seen from Figs. 9 and 10 that for angle of inclination of 135° and 180° the experimental results have lower values than the numerical results. This is because as the angle of inclination increases above 90° the base of the square cylinder which is made of plexiglass as mentioned before gets heated by the upward buoyant flow over the square cylinder and can no longer be treated as adiabatic as assumed in the numerical work.

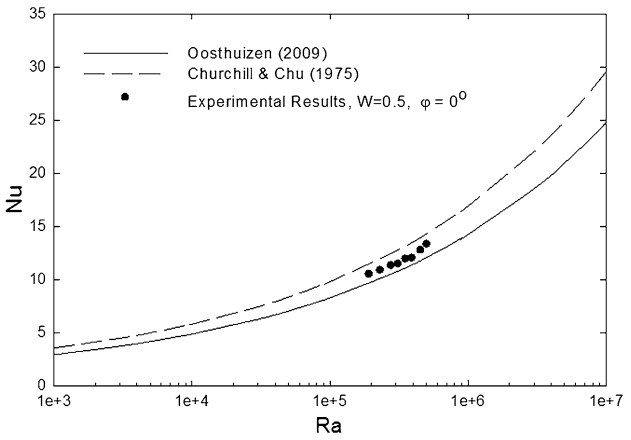

Fig. 5 Comparison of mean Nusselt number values given by correlation equations and experimental results for $W = 0.5$ and $\varphi = 0°$

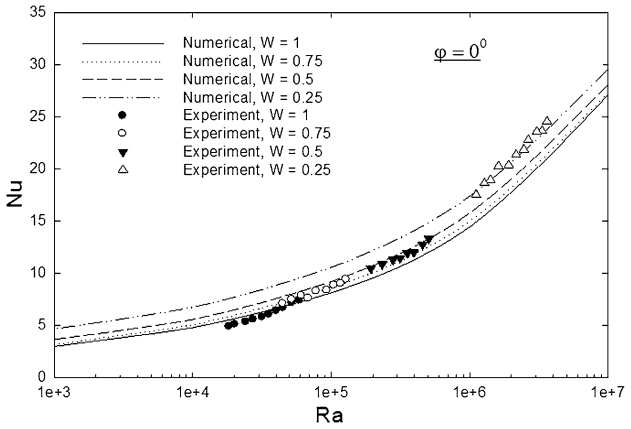

Fig. 6 Variation of mean Nusselt number for the square cylinder with Rayleigh number for various values of dimensionless cylinder width, *W*, when $\varphi = 0°$

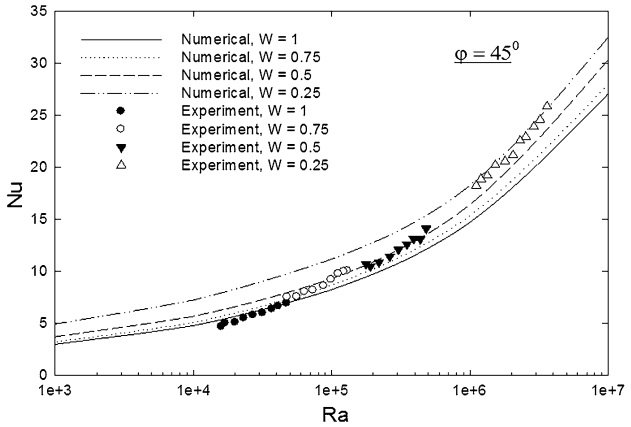

Fig. 7 Variation of mean Nusselt number for the square cylinder with Rayleigh number for various values of dimensionless cylinder width, *W*, when $\varphi = 45°$

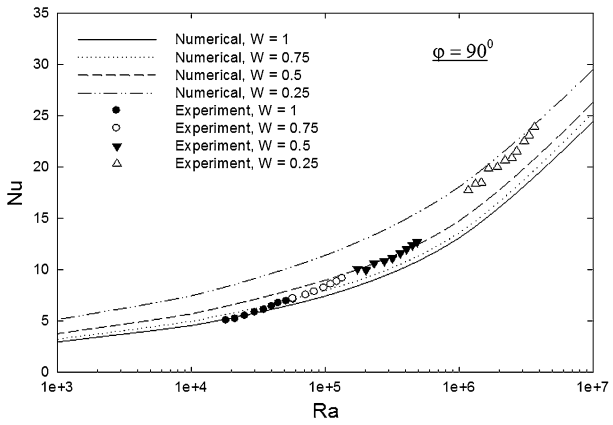

Fig. 8 Variation of mean Nusselt number for the square cylinder with Rayleigh number for various values of dimensionless cylinder width, *W*, when $\varphi = 90°$

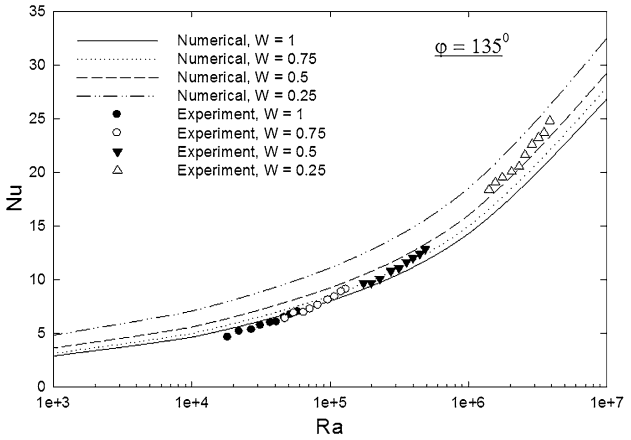

Fig. 9 Variation of mean Nusselt number for the square cylinder with Rayleigh number for various values of dimensionless cylinder width, *W*, when $\varphi = 135°$

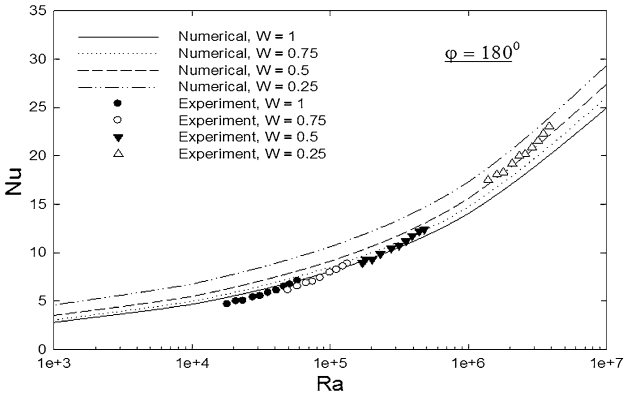

Fig. 10 Variation of mean Nusselt number for the square cylinder with Rayleigh number for various values of dimensionless cylinder width, *W*, when $\varphi = 180°$

Experimental results in the dimensionless form for different dimensionless width, W, and different angles of inclination are given in Tables 4, 5, 6 and 7.

Typical variations of the mean Nusselt number for the entire cylinder, *Nu*, with dimensionless cylinder width, *W*, for various values of *Ra* and φ are shown in Fig. 11. It will be seen from this figure that, the mean Nusselt number increases with decreasing *W* essentially at the lower values of *W* considered. At the lower values of *Ra* considered and when the dimensionless cylinder width, *W*, approximately greater than 0.6 the mean Nusselt number is essentially independent of the angle of inclination, φ. However at larger values of *Ra* the mean Nusselt number depends on the angle of inclination φ.

Figures 12 and 13 shows the variation of the mean Nusselt number with angle of inclination for different values of *W*. Figure 12 shows a good agreement between the numerical and the experimental results for inclination angles below 90° and that the experimental results have lower values than the numerical results as the angle of inclination gets larger than 90° as discussed before. Considering the numerical results given in Fig. 13 which shows the variation of the mean Nusselt number for the square cylinder with φ for various values of Rayleigh number and of the dimensionless cylinder width, *W*, it will clearly be seen that the mean Nusselt number at the lower values of Rayleigh numbers varies differently than at the higher values of the Rayleigh numbers. As already mentioned at the lower values of the Rayleigh number the mean Nusselt number is almost independent of the angle of inclination. However at higher values of Rayleigh number this is not the case. At the higher values of the Rayleigh number when dimensionless square cylinder width, *W*, is bigger than 0.25 the lowest mean Nusselt number occurs when the cylinder is in a horizontal position, i.e., when φ is equal 90° while the highest mean Nusselt number occurs when the cylinder is at inclination angles, φ, of 45° and 135°. When the dimensionless square cylinder width, *W*, is equal to 0.25 the lowest mean Nusselt number occurs when the cylinder is in a vertical position, i.e., when φ is equal 0° and 180° while

Table 4 Experimental results for $W = 1$

φ = 0°		φ = 45°		φ = 90°		φ = 135°		φ = 180°	
Ra	Nu	Ra	Nu	Ra	Nu	Ra	Nu	Ra	Nu
5.887E+04	7.37	5.667E+04	7.456	5.826E+04	7.062	5.863E+04	7.003	5.840E+04	7.061
5.224E+04	7.155	4.747E+04	6.9	5.163E+04	6.895	5.192E+04	6.722	5.150E+04	6.693
4.508E+04	6.67	4.124E+04	6.63	4.504E+04	6.72	4.680E+04	6.448	4.670E+04	6.464
4.022E+04	6.39	3.708E+04	6.36	4.020E+04	6.39	4.115E+04	6.04	4.120E+04	6.08
3.569E+04	6.034	3.169E+04	5.98	3.510E+04	6.056	3.715E+04	5.965	3.580E+04	5.825
3.184E+04	5.79	2.710E+04	5.77	3.004E+04	5.81	3.151E+04	5.693	3.130E+04	5.5
2.730E+04	5.544	2.323E+04	5.482	2.530E+04	5.48	2.714E+04	5.31	2.780E+04	5.353
2.420E+04	5.317	2.009E+04	5.07	2.137E+04	5.18	2.211E+04	5.153	2.350E+04	5
2.015E+04	5.09	1.703E+04	5	1.830E+04	5.03	1.828E+04	4.61	2.100E+04	4.951
1.830E+04	4.88	1.594E+04	4.66	–	–	–	–	1.810E+04	4.641

Table 5 Experimental results for $W = 0.75$

φ = 0°		φ = 45°		φ = 90°		φ = 135°		φ = 180°	
Ra	Nu	Ra	Nu	Ra	Nu	Ra	Nu	Ra	Nu
1.281E+05	9.39	1.303E+05	10.034	1.350E+05	9.121	1.304E+05	9.071	1.340E+05	8.844
1.176E+05	8.994	1.227E+05	9.951	1.231E+05	8.787	1.211E+05	8.837	1.247E+05	8.565
1.050E+05	8.834	1.121E+05	9.745	1.107E+05	8.55	1.086E+05	8.374	1.120E+05	8.217
9.330E+04	8.353	9.955E+04	9.188	9.852E+04	8.186	9.701E+04	8.072	1.003E+05	7.933
7.834E+04	8.284	8.801E+04	8.585	8.340E+04	7.83	8.211E+04	7.59	8.526E+04	7.37
6.834E+04	7.575	7.350E+04	8.163	7.205E+04	7.51	7.210E+04	7.23	7.500E+04	6.973
6.109E+04	7.832	6.387E+04	8.02	5.780E+04	7.155	6.480E+04	6.922	6.766E+04	6.833
5.211E+04	7.455	5.618E+04	7.54	–	–	5.500E+04	6.851	5.820E+04	6.5
4.471E+04	7.065	4.783E+04	7.51	–	–	4.756E+04	6.344	4.970E+04	6.09

Table 6 Experimental results for $W = 0.5$

φ = 0°		φ = 45°		φ = 90°		φ = 135°		φ = 180°	
Ra	Nu	Ra	Nu	Ra	Nu	Ra	Nu	Ra	Nu
5.067E+05	13.292	4.830E+05	14.091	4.877E+05	12.684	4.866E+05	12.843	4.798E+05	12.395
4.570E+05	12.74	4.380E+05	13.086	4.491E+05	12.39	4.453E+05	12.4114	4.418E+05	12.194
3.950E+05	11.983	3.917E+05	13.107	4.056E+05	12	3.975E+05	12.024	3.933E+05	11.721
3.547E+05	11.905	3.508E+05	12.59	3.646E+05	11.582	3.568E+05	11.647	3.543E+05	11.205
3.142E+05	11.435	3.045E+05	12.073	3.184E+05	11.12	3.143E+05	11.065	3.152E+05	10.721
2.790E+05	11.286	2.633E+05	11.404	2.771E+05	10.821	2.751E+05	10.815	2.766E+05	10.44
2.332E+05	10.842	2.198E+05	10.864	2.322E+05	10.611	2.285E+05	10.1	2.310E+05	9.87
1.936E+05	10.47	1.906E+05	10.467	2.024E+05	9.944	1.983E+05	9.71	2.014E+05	9.272
–	–	1.772E+05	10.69	1.745E+05	10.064	1.747E+05	9.672	1.808E+05	9.312
–	–	–	–	–	–	–	–	1.715E+05	8.931

Table 7 Experimental results for $W = 0.25$

φ = 0°		φ = 45°		φ = 90°		φ = 135°		φ = 180°	
Ra	Nu	Ra	Nu	Ra	Nu	Ra	Nu	Ra	Nu
3.617E+06	24.512	3.611E+06	25.843	3.663E+06	23.89	3.873E+06	24.8	3.856E+06	23.04
3.331E+06	23.611	3.218E+06	24.563	3.333E+06	23.082	3.524E+06	23.7	3.497E+06	22.27
3.050E+06	23.531	2.904E+06	23.894	3.064E+06	22.5	3.212E+06	23.244	3.201E+06	21.55
2.649E+06	22.744	2.533E+06	22.923	2.693E+06	21.524	2.880E+06	22.61	2.890E+06	20.85
2.460E+06	21.835	2.306E+06	22.544	2.478E+06	20.88	2.560E+06	21.612	2.580E+06	20.18
2.165E+06	21.315	2.052E+06	21.16	2.201E+06	20.631	2.324E+06	20.541	2.350E+06	20
1.914E+06	20.334	1.796E+06	20.58	1.936E+06	19.97	2.050E+06	20.06	2.079E+06	19.19
1.617E+06	20.226	1.527E+06	20.21	1.659E+06	19.825	1.760E+06	19.516	1.796E+06	18.29
1.412E+06	18.93	1.335E+06	19.2	1.466E+06	18.462	1.564E+06	19.06	1.612E+06	18.05
1.276E+06	18.6	1.202E+06	18.86	1.326E+06	18.326	1.408E+06	18.39	1.391E+06	17.475

the highest mean Nusselt number occurs when the cylinder is at inclination angles, φ, of between 45° and 135°.

In some situations the mean heat transfer rates from the individual surfaces, i.e., the left side, the right side, the front, and the top surfaces of the cylinder are of importance and these will be considered next. Typical variations of the mean Nusselt numbers for the front, right side, left side, and top surfaces with angles of inclination of various values of W and Ra are shown in Figs. 14, 15, 16 and 17, respectively.

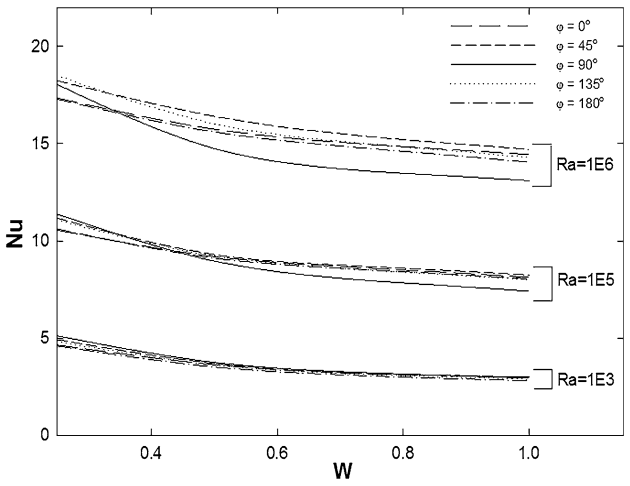

Fig. 11 Variation of mean Nusselt number for the cylinder with dimensionless cylinder width for various values of Rayleigh number and φ

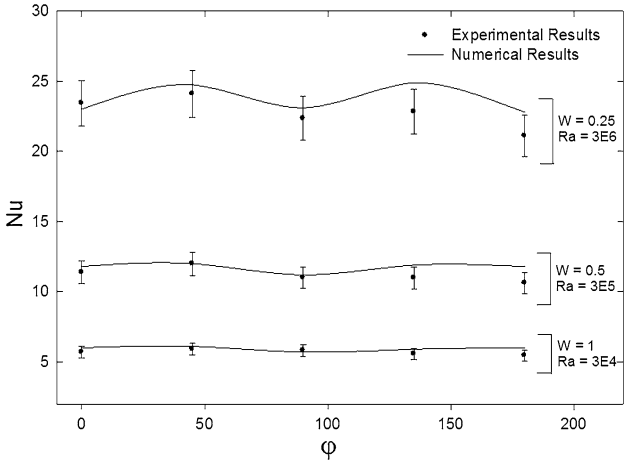

Fig. 12 Variation of mean Nusselt number for the cylinder with φ for various values of Rayleigh number and dimensionless cylinder width, W

Figure 14 shows that Nu_{front} increases as the dimensionless cylinder width W decreases and that the variation of Nu_{front} with φ at lower values of Rayleigh number differs from the variation at higher values of Rayleigh number. At lower values of Rayleigh number Nu_{front} has a maximum value when the inclination angle φ is equal to 90° and a minimum value when φ is equal to 180° whereas at higher values of Rayleigh number the maximum value of Nu_{front} occurs when the angle of inclination φ is equal to 45° while the lowest value again occurs when the angle of inclination φ is equal to 180°. It will be noted that at the highest value of Ra considered in Fig. 14, Nu_{front} increases as φ increases from 0° to 45°. Nu_{front} then decreases, as φ increases from 45° to 90°, then increases as φ increases from 90° to 135°, and then again decreases as φ increases from 135° to 180°. When dimensionless square cylinder

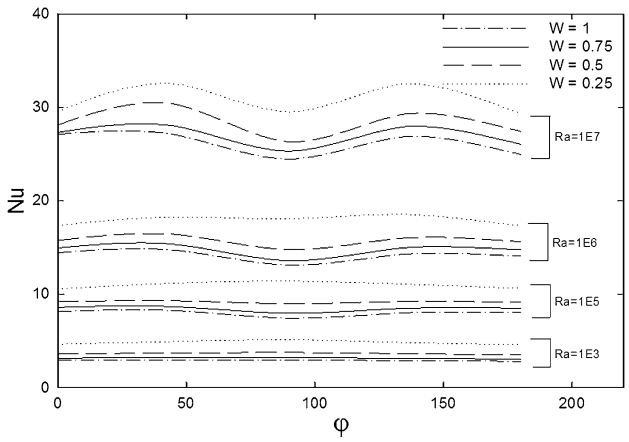

Fig. 13 Variation of mean Nusselt number for the cylinder with φ for various values of Rayleigh number and dimensionless cylinder width W

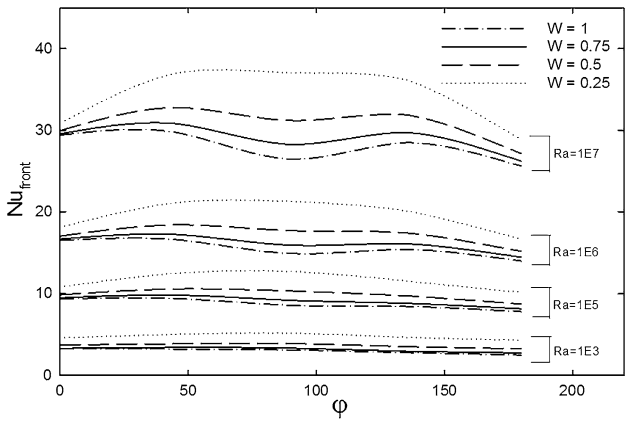

Fig. 14 Variation of mean Nusselt number for *front* side heated surface of the cylinder with φ for various values of Rayleigh number and dimensionless cylinder width W

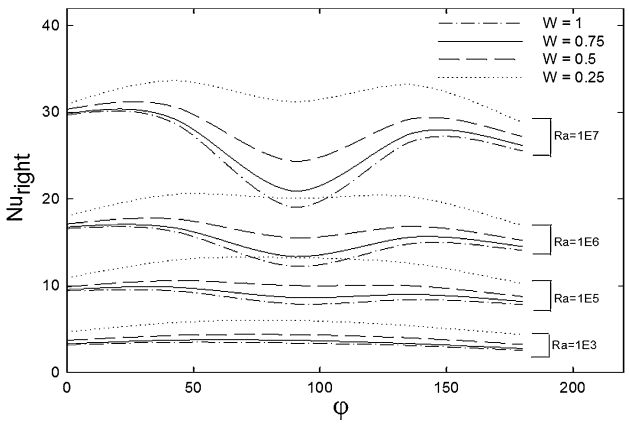

Fig. 15 Variation of mean Nusselt number for *left* side heated surface of the cylinder with φ for various values of Rayleigh number and dimensionless cylinder width W

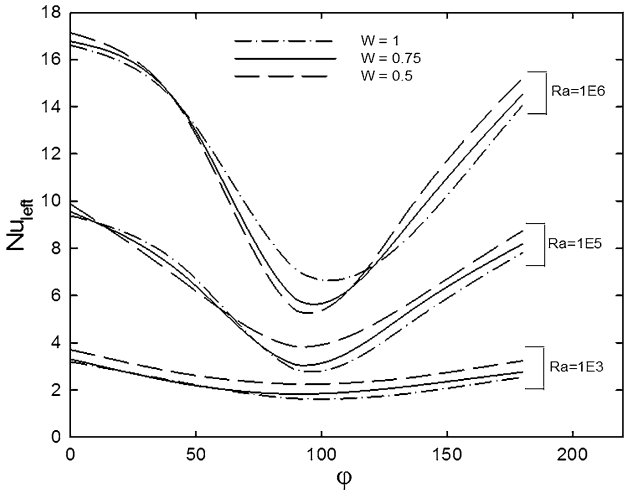

Fig. 16 Variation of mean Nusselt number for the *left* heated surface of the cylinder with φ for various values of the Rayleigh number and of the dimensionless cylinder width W

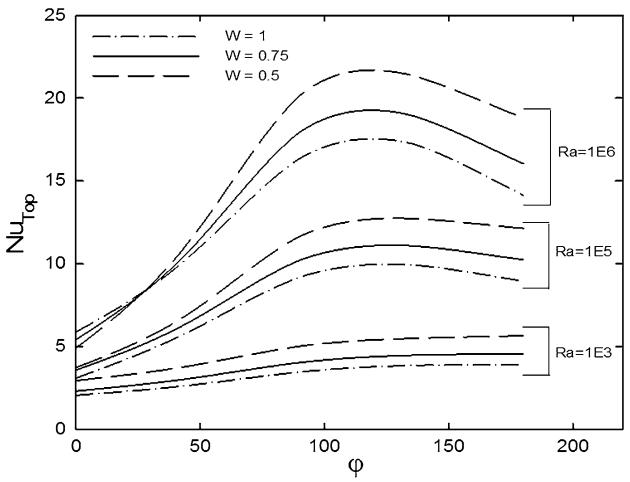

Fig. 17 Variation of mean Nusselt number for *top* side heated surface of the cylinder with φ for various values of Rayleigh number and dimensionless cylinder width W

width, W, is equal to 0.25 the maximum mean Nusselt number occurs when the cylinder is in a horizontal position, i.e., when φ is equal 90°. The results given in Fig. 15 shows that the variation of Nu_{right} with φ exhibits the same basic form of behavior as Nu_{front} (Fig. 14), except that at the highest Rayleigh number considered when dimensionless square cylinder width,W, is equal to 0.25 the maximum mean Nusselt number occurs when φ is equal 45° and 135°.

Figure 16 shows the variation of Nu_{left} with φ for various values of Ra and W. It will be seen that at lower Rayleigh numbers Nu_{left} increases as the dimensionless plate width W decreases at all angles of inclination. However at higher Rayleigh numbers a different form of variation of Nu_{left} with W exists. At high Rayleigh numbers Nu_{left} increases as the dimensionless plate width W decreases for values of φ near 0° and 180° but decreases as the dimensionless plate width W decreases for values of φ near 90° This is because as the angle of inclination of the cylinder increases 0° the left side of the cylinder changes from being an effective vertical flat plate to being horizontal plate for φ near 90° and then again become an effective vertical flat plate for φ near 180°.

The changes in the Nusselt number of the individual surfaces is further illustrated by the results given in Fig. 17 which shows that the Nu_{Top} increases as the dimensionless cylinder width W decreases at all angles of inclination except at the highest Rayleigh number considered when at angles of inclination φ near to 0° where Nu_{Top} increases as the dimensionless plate width W increases. It should also be noted that at the lower values of Rayleigh number considered Nu_{Top} increases continuously as the angle of inclination increases. However at higher values of Rayleigh number Nu_{Top} increases as the angle of inclination increases but then passes through a maximum at an angle of inclination φ of about 120° and then decreases with a further increase in φ.

Typical variations of Nu_{Top}, Nu_{front}, Nu_{right}, and Nu_{left}, with an angle of inclination φ and for two values of Ra and W equal 0.5 are shown in Figs. 18 and 19. Nu_{front}, Nu_{right}, and Nu_{left}, have the same values when the angle of inclination is equal to 0° and to 180°. As expected, it will be seen that Nu_{Top} is much less than Nu_{front}, Nu_{right}, and Nu_{left} when the angle of inclination is equal to 0°. However as the angle of inclination increases this difference decreases and for angles greater than about 75° the Nu_{Top} is greater than Nu_{front}, Nu_{right}, and Nu_{left}. These changes arise from the fact that as the angle of inclination of each of the surfaces relative to the vertical changes, e.g., when the angle of inclination of the cylinder is 0° the 'top' surface faces upwards

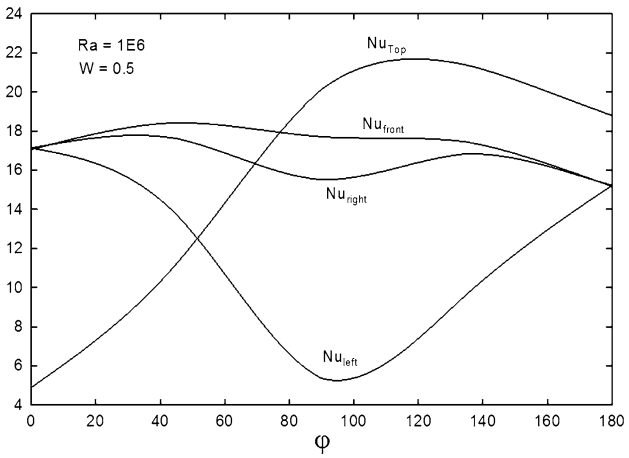

Fig. 18 Variation of mean Nusselt number for surfaces that make up the cylinder, *top*, *front*, *right* and *left* with φ for $Ra = 10^6$ and for $W = 0.5$

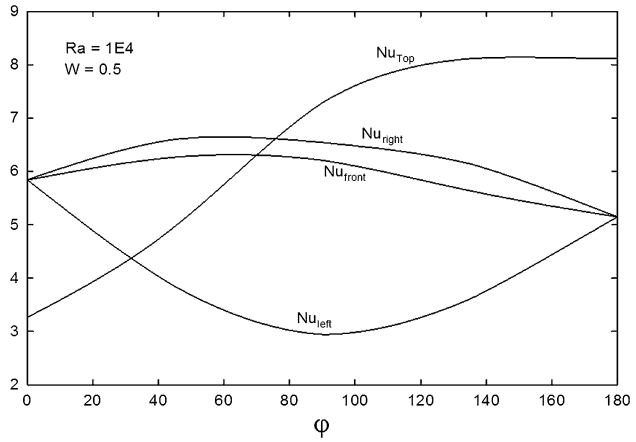

Fig. 19 Variation of mean Nusselt number for surfaces that make up the cylinder, *top*, *front*, *right* and *left* with φ for $Ra = 10^4$ and for $W = 0.5$

whereas when the angle of inclination of the cylinder is 180° the 'top' surface faces downwards.

The changes in the three-dimensional flow patterns and the flow interaction between the surfaces that make up the square cylinder with angle of inclination on the top surface of the square cylinder are illustrated by the local Nusselt number distributions over the heated plate as shown in Fig. 20, where the dimensionless local Nusselt number are defined as:

$$Nu_{L(Top)} = \frac{q'_{Top}\, h}{k(T_w - T_F)} \tag{20}$$

This figure shows the local Nusselt number distributions over the top surface of the square cylinder for W equal to 0.5 and two values of Rayleigh numbers for different angles of inclination. The results given in this figure illustrate how the angle of inclination and the interaction of flow at different Rayleigh numbers have an effect on the top surface as the result of interaction of flow over the surfaces that make up the square cylinder and how they significantly have different behavior on the top surface as the Rayleigh numbers and angle of inclination changes which gives rise to a complex flow over the top surface. This figure shows regions of high and low local Nusselt number for different inclination angle and different Rayleigh numbers.

The variation of the mean Nusselt number for the top surface relative to the mean Nusselt numbers for the other surfaces has already been discussed. The relative importance of the heat transfer rate from the top surface compared to that from the vertical side surfaces of the cylinder will however depend both on the mean Nusselt numbers for the surfaces and the relative surface areas. Now since:

$$A_{side} = 4W, \quad A_{Top} = W^2, \quad \text{and} \quad A_{total} = 4W + W^2 \tag{21}$$

where A_{total}, A_{side}, and A_{Top} are the dimensionless surface areas of the entire cylinder, of all of the 'sides' of the

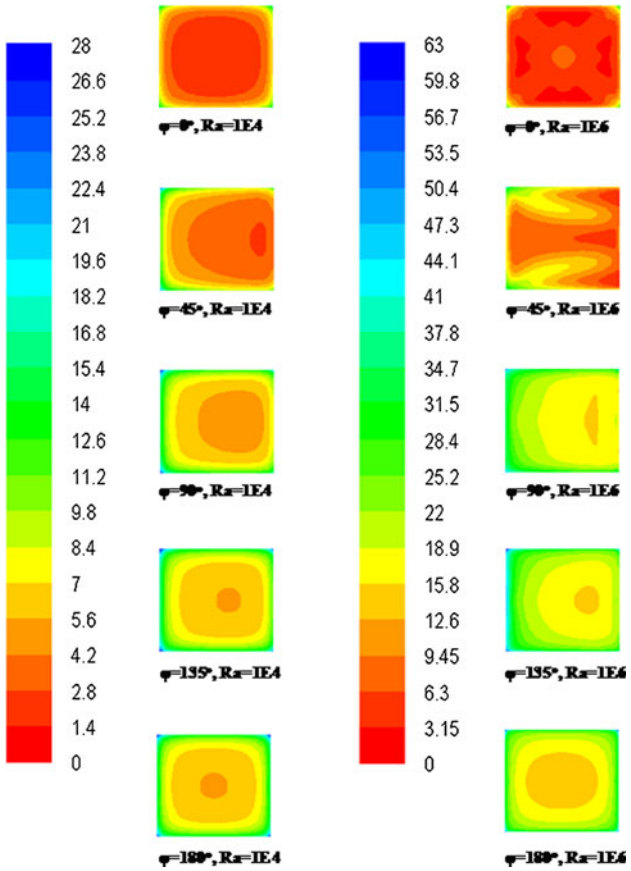

Fig. 20 Variation of local Nusselt number based on h over *top* side of the square cylinder with different angle of inclinations for Ra = 1E4, Ra = 1E6 and $W = 0.5$

cylinder, and of the 'top' surface of the cylinder respectively, it follows that:

$$\frac{A_{side}}{A_{total}} = \frac{4}{4 + W}, \quad \frac{A_{Top}}{A_{total}} = \frac{W}{4 + W}, \quad \frac{A_{Top}}{A_{side}} = \frac{W}{4} \tag{22}$$

This equation indicates that over the range of values of W considered here, i.e., 0.25 to 1, A_{Top}/A_{side} is relatively small having a maximum value of 0.25 when $W = 1$, i.e., the area of the top surface relative to the area of the vertical side surfaces remains comparatively small.

Now:

$$\frac{Q_{total}}{Q_{Top}} = \frac{q' A_{total}}{q'_{Top} A_{Top}} = \frac{Nu A_{total}}{Nu_{Top} A_{Top}} = \frac{Nu}{Nu_{Top}} \frac{4 + W}{W} \tag{23}$$

This equation allows Q_{total}/Q_{Top} to be found using the calculated Nusselt number values. Some typical results obtained are shown in Fig. 21. From these results it will be seen that while Q_{total}/Q_{Top} is always greater than approximately 4 it is only at low values of φ that the contribution of Q_{Top} to Q_{total} can be neglected. The assumption that the contribution of Q_{Top} to Q_{total} can be

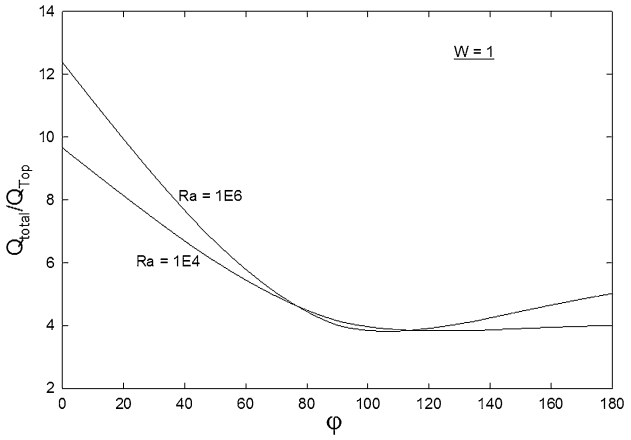

Fig. 21 Variation of the ratio of the total heat transfer rate from the surface of the cylinder to the heat transfer rate from the *top* surface with angle of inclinations for *Ra* values of 10^4 and 10^6 and for $W = 1$

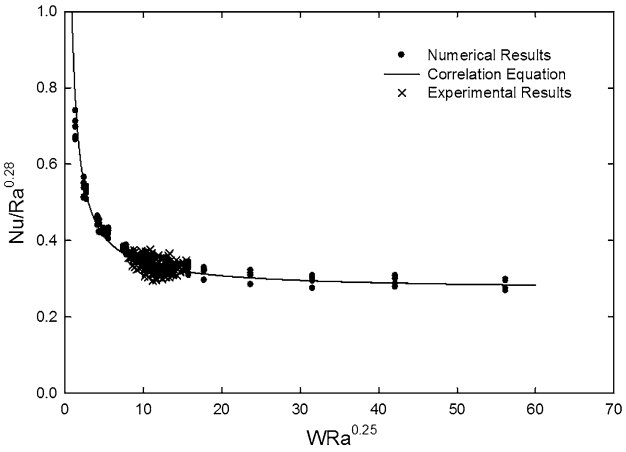

Fig. 22 Comparison of correlation equation with the numerical and experimental for inclined square cylinder with exposed *top* surface

neglected has sometimes been used in deriving correlation equations for the heat transfer rate from vertical square cylinders using:

$$Nu = Nu_{side}\left(\frac{A_{side}}{A_{total}}\right) + Nu_{top}\left(\frac{A_{Top}}{A_{total}}\right) \quad (24)$$

and neglecting the second term on the right hand side. The present results show that this approach will not normally be applicable to the inclined cylinder case.

The surfaces that make up the square cylinder are of the form of flat plates connected to each other. The correlation equation for the case of a wide flat plate with a uniform surface temperature has the form:

$$Nu_0 = \mathrm{B}\, Ra^{0.25} \quad (25)$$

The parameter B depending only on the Prandtl number of the fluid involved. When the width of the plate becomes relatively small and inclined at an angle to the vertical edge effects become important (see Kalendar and Oosthuizen [46]) and the Nusselt number depends on the boundary layer thickness to plate width ratio, i.e., since the boundary layer thickness will be dependent on the value of:

$$\varepsilon = \frac{h}{wRa^{0.25}} = \frac{1}{WRa^{0.25}} \quad (26)$$

The Nusselt number will of course also be dependent on the inclination angle. Therefore when the surfaces that make up the square cylinder are narrow and inclined at an angle to the vertical, the heat transfer rate from the square cylinder is given by an equation of the form:

$$\frac{Nu}{Ra^{0.25}} = \text{constant} + \text{function}\ (Ra,\ W,\ \varphi) \quad (27)$$

Using an equation of this form it has been found that the present results for the case of a heated square cylinder with

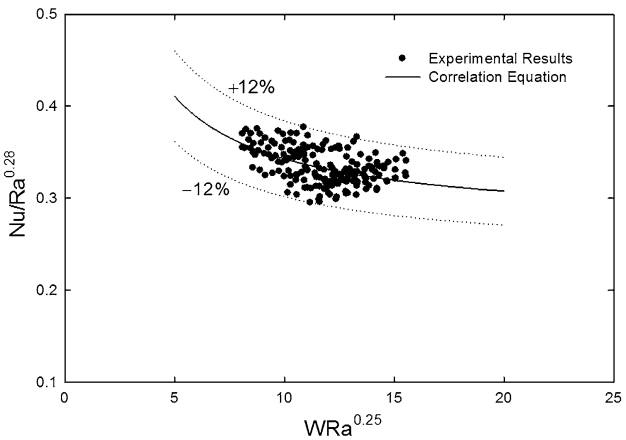

Fig. 23 Comparison of correlation equation with the experimental results for inclined square cylinder with exposed *top* surface

an exposed top surface and inclined at an angle, φ, of between $\varphi = 0°$ and $\varphi = 180°$, and with different dimensionless widths can be approximately described by:

$$\frac{Nu_{memp}}{Ra^{0.28}} = 0.27 + \frac{0.65}{(WRa^{0.25})^{0.95}} \quad (28)$$

The index on the left hand side of Eq. (28) has a Rayleigh number to the power of 0.28 instead of 0.25 since the interaction of flow over the plates that make up the square cylinder become more important as the plate width decreases. A comparison of the results given by this correlation Eq. (28) with the numerical and experimental results is shown in Fig. 22. It will be seen that the equation describes the computed numerical results to an accuracy of better than 92 %. Figure 23 shows the comparison of the experimental results with the correlation Eq. (28), the

agreement being to an accuracy of better than 86 %, where the 12 % in Fig. 23 shows the 95 % prediction band of the experimental results.

5 Conclusions

Natural convective heat transfer from an isothermal inclined square cylinder which have an exposed top surface and is, in general, inclined at an angle to the vertical between vertically upwards and vertically downwards has been numerically and experimentally studied. The effects of Dimensionless widths, Rayleigh numbers, and inclination angles on the mean Nusselt number for the entire cylinder and for the mean Nusselt numbers for the various surfaces that make up the cylinder were conducted in this study. The results of the present study indicate that:

1. The experimental results are in a good agreement with the numerical results for square cylinder for all angle of inclination considered in this study.
2. The mean Nusselt number for the cylinder increases with decreasing W under all conditions considered.
3. The relative magnitudes of the mean Nusselt numbers for the various faces that make up the cylinder vary considerably with the inclination angle and as a result it is only possible to neglect the heat transfer from the 'top' surface compared to that from the other surfaces when the dimensionless width is small and the angle of inclination is near 0°.
4. At lower values of Ra (approximately less than 10^4) for all dimensionless plate widths, W, considered the mean Nusselt number is independent of angle of inclination φ. At larger values of Ra the dependence of the mean Nusselt number on the angle of inclination φ becomes significant.
5. At the higher values of Rayleigh number the lowest mean Nusselt number occurs when the cylinder is in a horizontal position, i.e., when φ is equal 90° while the highest mean Nusselt number occurs when the cylinder is at inclination angles, φ, of 45° and 135°.
6. The results for the mean Nusselt number based on the mean heat transfer rate from vertical and inclined square cylinder can be adequately correlated by the Eq. (28).

Acknowledgments This work was supported by the Public Authority for Applied Education and Training of Kuwait and the Natural Sciences and Engineering Research Council of Canada.

References

1. Ede AJ (1967) Advances in free convection. Adv Heat Transf 4:1–64
2. Burmeister LC (1983) Convective heat transfer. Wiley, New York
3. Jaluria Y (1980) Natural convection, 1st edn. Pergamon Press, Oxford
4. Cebeci T (1974) Laminar free convective heat transfer from the outer surface of a vertical slender circular cylinder. In: Proceedings of 5th international heat transfer conference, society of heat transfer of Japan, vol 3. Tokyo, Japan, Paper NC 1.4, pp 15–19
5. Lee HR, Chen TS, Armaly BF (1988) Natural convection along slender vertical cylinders with variable surface temperature. J Heat Transf Trans ASME 110(1):103–108
6. Le Fevre EJ, Ede AJ (1956) Laminar free convection from the outer surface of a vertical circular cylinder. In: Proceedings 9th international congress applied mechanics Brussels, vol 4. pp 175–183
7. Crane LJ (1976) Natural convection from a vertical cylinder at very large Prandtl numbers. J Eng Math 10(2):115–124
8. Kimura F, Tachibana T, Kitamura K, Hosokawa T (2004) Fluid flow and heat transfer of natural convection around heated vertical cylinders (effect of cylinder diameter). JSME Int J Ser B Fluids Therm Eng 47(2):156–161
9. Oosthuizen PH (2007) Natural convective heat transfer from an isothermal vertical cylinder with an exposed upper surface mounted on a flat adiabatic base. In: Proceedings ASME international mechanical engineering congress and exposition, IMECE, Seattle, Washington, USA, November 2007, Paper IMECE2007-42711, pp 389–395
10. Oosthuizen PH (1979) Free convective heat transfer from vertical cylinders with exposed ends. Trans Can Soc Mech Eng 5(4): 231–234
11. Jarall S, Campo A (2005) Experimental study of natural convection from electrically heated vertical cylinders immersed in air. Exp Heat Transf 18(3):127–134
12. Welling I, Koskela H, Hautalampi T (1998) Experimental study of the natural-convection plume from a heated vertical cylinder. Exp Heat Transf 11(2):135–149
13. Fukusawa K, Iguchi M (1962) On optical measurements of natural convection along vertical cylinder. J Mech Lab Jpn 16(3): 114–120
14. Oosthuizen PH (2007) Natural convective heat transfer from a vertical cylinder with an exposed upper surface. In: ASME/JSME thermal engineering summer heat transfer conference, ASME, Vancouver, BC, Canada, pp 489–495
15. Oosthuizen PH, Paul JT (2008) Natural convective heat transfer from an isothermal cylinder with an exposed upper surface mounted on a flat adiabatic base with a flat adiabatic surface above the cylinder. In: EUROTHERM, 5th European thermal science conference, Eindhoven, Netherlands
16. Koch W (1927) Heat transmission from hot pipes. Beih. Gesundh. Ingr. 22:1–27
17. Farber EA, Rennat HO (1957) Variation of heat transfer coefficient with length-inclined tubes in still air. Ind Eng Chem 49(3):437–440
18. Eckert ER (1959) Heat and mass transfer, 2nd edn. McGraw-Hill, New York
19. Oosthuizen PH (1976) Experimental study of free convective heat transfer from inclined cylinders. J Heat Transf 98(4):672
20. Al-Arabi M, Salman YK (1980) Laminar natural convection heat transfer from an inclined cylinder. Int J Heat Mass Transf 23(1):45–51

21. Al-Arabi M, Khamis M (1982) Natural convection heat transfer from inclined cylinders. Int J Heat Mass Transf 25(1):3–15
22. Chand J, Vir D (1980) A unified approach to natural convection heat transfer in the laminar region from horizontal and inclined cylinders. Lett Heat Mass Trans 7(3):213–225
23. Oosthuizen PH, Mansingh V (1983) Free and forced convective heat transfer from short cylinders. In: Joint ASME/AIChE national heat transfer conference ASME, Seattle, WA, USA, July 1983
24. Oosthuizen PH, Paul JT (1991) Natural convective heat transfer from inclined downward pointing cylinders with exposed ends. In: Proceedings of the world conference on experimental heat transfer, fluid mechanics, and thermodynamics. pp 697
25. Popiel CO, Wojtkowiak J (2004) Experiments on free convective heat transfer from side walls of a vertical square cylinder in air. Exp Therm Fluid Sci 29(1):1–8
26. Al-Arabi M, Sarhan A (1984) Natural convection heat transfer from square cylinders. Appl Sci Res 41(2):93–104
27. Oosthuizen PH (2008) Natural convective heat transfer from an isothermal vertical square cylinder mounted on a flat adiabatic base. In: ASME summer heat transfer conference, ASME, Jacksonville, FL, United states, August 2008, pp 499–505
28. Starner KE, McManus HN (1963) An experimental investigation of free convection heat transfer from rectangular fin arrays. J Heat Trans 85:273–278
29. Welling JR, Wooldridge CR (1965) Free convection heat transfer coefficients from rectangular vertical fins. J Heat Trans 87:439–444
30. Harahap F, McManus HN (1967) Natural convection heat transfer from horizontal rectangular fin array. J Heat Transfer 89:32–38
31. Leung CW, Probert SD, Shilton MJ (1986) Heat transfer performance of vertical rectangular fins protruding from bases (Effect of fin length). Appl Energy 22:313–318
32. Leung CW, Probert SD (1989) Thermal effectiveness of short-protrusion rectangular heat exchanger fins. Appl Energy 34:1–8
33. Yuncu H, Anbar G (1998) An experimental investigation on performance of rectangular fins on a horizontal base in free convection heat transfer. Heat Mass Transf 33:507–514
34. Mobedi M, Yuncu H (2003) A three dimensional numerical study on natural convection heat transfer from short horizontal rectangular fin array. Heat Mass Transf 39:267–275
35. Harahap F, Rudianto E (2005) Measurements of steady-state heat dissipation from miniaturized horizontally-based straight rectangular fin arrays. Heat Mass Transfer 41:280–288
36. Sahray D, Magril R, Dubovsky V, Ziskind G, Letan R (2006) Natural convection heat transfer from pin fin heat sinks with internal base. In: Proceedings of 13th international heat transfer conference, Sydney, Australia
37. Harahap F, Lesmana H, Dirgayasa S (2006) Measurements of heat dissipation from miniaturized vertical rectangular fin arrays. Heat Mass Transf 42:1025–1036
38. Yazicioglu B, Yancu H (2007) Optimum fin spacing of rectangular fins on a vertical base in free convection heat transfer. J Heat Mass Transf 44:11–21
39. Sahray D, Magril R, Dubovsky V, Ziskind G, Letan R (2007) Study of horizontal-base pin-fin heat sinks in natural convection. In: Proceedings of ASME InterPACK, Vancouver, British Columbia, Canada, July 2007, pp 925–931
40. Kalendar A, Oosthuizen PH (2009) Natural convective heat transfer from an inclined isothermal square cylinder with an exposed top surface mounted on a flat adiabatic base. In: Proceedings of the ASME heat transfer summer conference, San Francisco, California USA, July 2009, HT2009-88094, pp 115–122
41. Kalendar A, Oosthuizen PH, Alhadhrami A (2010) Experimental study of natural convective heat transfer from an inclined isothermal square cylinder with an exposed top surface mounted on a flat adiabatic base. In: Proceeding of the International heat transfer conference IHTC14, Washington, DC, USA, August 2010, Paper IHTC14-22846, pp 113–120
42. Kalendar A (2011) Numerical and experimental studies of natural convective heat transfer from vertical and inclined flat plates and short cylinders. PHD thesis, Queen's University, Kingston, Canada
43. Moffat RJ (1983) Using uncertainty analysis in the planning of an experiment. Trans ASME J Fluids Eng 107(2):173–178
44. Moffat RJ (1988) Describing the uncertainties in experimental results. Elsevier Sci Publ Exp Therm Fluid Sci 1:3–17
45. Churchill SW, Chu HHS (1975) Correlating equations for laminar and turbulent free convection from a vertical plate. Int J Heat Mass Transf 18:1323–1329
46. Kalendar A, Oosthuizen PH (2011) Numerical and experimental studies for natural convective heat transfer from vertical and inclined narrow isothermal flat plates. Heat Mass Transfer 47:1181–1195